Whole-body MRI: comprehensive evaluation on a 48-channel 3T MRI system in less than 40 minutes. Preliminary results*

RM de corpo inteiro: avaliação de protocolo em equipamento 3T com 48 canais em menos de 40 minutos. Resultados preliminares

Mateus de Andrade Hernandes[1], Richard C. Semelka[2], Jorge Elias Júnior[3], Saraporn Bamrungchart[1], Brian M. Dale[4], Clifton Stallings[5]

Abstract **Objective:** To evaluate a comprehensive MRI protocol that investigates for cancer, vascular disease, and degenerative/inflammatory disease from the head to the pelvis in less than 40 minutes on a new generation 48-channel 3T system. **Materials and Methods:** All MR studies were performed on a 48-channel 3T MR scanner. A 20-channel head/neck coil, two 18-channel body arrays, and a 32-channel spine array were employed. A total of 4 healthy individuals were studied. The designed protocol included a combination of single-shot T2-weighted sequences, T1-weighted 3D gradient-echo pre- and post-gadolinium. All images were retrospectively evaluated by two radiologists independently for overall image quality. **Results:** The image quality for cancer was rated as excellent in the liver, pancreas, kidneys, lungs, pelvic organs, and brain, and rated as fair in the colon and breast. For vascular diseases ratings were excellent in the aorta, major branch vessel origins, inferior vena cava, portal and hepatic veins, rated as good in pulmonary arteries, and as poor in the coronary arteries. For degenerative/inflammatory diseases ratings were excellent in the brain, liver and pancreas. The inter-observer agreement was excellent. **Conclusion:** A comprehensive and time efficient screening for important categories of disease processes may be achieved with high quality imaging in a new generation 48-channel 3T system.
Keywords: Whole-body MRI; Screening; Protocol; Preliminary results; 3 tesla.

Resumo **Objetivo:** Avaliar protocolo de RM para investigação de neoplasia, doenças vascular e degenerativa/inflamatória da cabeça à pelve em menos de 40 minutos em equipamento 3T com 48 canais. **Materiais e Métodos:** Todos os exames foram realizados em equipamento 3T com 48 canais. Foram utilizadas bobinas de cabeça/pescoço (20 canais), duas de corpo interligadas (18 canais) e uma de coluna (32 canais). Quatro voluntários saudáveis foram estudados. Foi utilizado protocolo com sequências *single shot* pesadas em T2 e gradiente-eco 3D pesadas em T1 pré e pós-gadolínio. Todas as imagens foram avaliadas quanto à qualidade, retrospectivamente, por dois radiologistas de forma independente. **Resultados:** A qualidade da imagem foi classificada como excelente para o fígado, pâncreas, rins, pulmões, órgãos pélvicos e encéfalo, e como adequada para cólon e mamas. Para as doenças vasculares as imagens foram classificadas como excelentes para aorta e seus ramos principais, veia cava inferior, veias porta e hepáticas, como boas para artérias pulmonares, e como inadequadas para coronárias. As classificações para doenças degenerativas/inflamatórias foram excelente no encéfalo, fígado e pâncreas. A concordância interobservador foi excelente. **Conclusão:** Um rastreamento abrangente de importantes categorias de doenças pode ser realizado utilizando imagens de alta qualidade obtidas em uma nova geração de equipamento 3T com 48 canais.
Unitermos: RM de corpo inteiro; *Screening*; Protocolo; Resultados preliminares; 3 tesla.

Hernandes MA, Semelka RC, Elias Jr J, Bamrungchart S, Dale BM, Stallings C. Whole-body MRI: comprehensive evaluation on a 48-channel 3T MRI system in less than 40 minutes. Preliminary results. Radiol Bras. 2012 Nov/Dez;45(6):319–325.

INTRODUCTION

The concept of whole-body MRI is not new, however its clinical use has been limited in the past mainly because of its long scanning time and/or poor image quality. Additionally, there has been progress in the development of other whole-body imaging modalities, such as whole-body CT, PET, and PET/CT. Recently, however, an increasing awareness of the risks of ionizing radiation exposure has encouraged the investigation of alternative imaging techniques[1,2].

Since its early description, whole-body MRI has been considered a promising tool for detection of disease. The greater intrinsic soft tissue contrast resolution and greater sensitivity for intravenous contrast of MRI over CT, allied with the lack of radiation exposure and safer contrast materials, make MRI an excellent choice for screening purposes. However, whole-body MRI with surface coils and conventional sequences is time consuming and costly. The introduction of faster gradient MRI systems, parallel acquisition strategies, re-

* Study developed at Department of Radiology, University of North Carolina, Chapel Hill, NC, USA.

1. MDs, Research Fellows, Department of Radiology, University of North Carolina, Chapel Hill, NC, USA.

2. MD, Professor, Department of Radiology, University of North Carolina, Chapel Hill, NC, USA.

3. MD, PhD, Professor, Imaging and Medical Physics Center, School of Medicine of Ribeirão Preto, University of São Paulo, Ribeirão Preto, SP, Brazil.

4. PhD, Siemens Medical Solutions USA, Inc., Cary, NC, USA.

5. RTS, MRI Chief Technologist, Department of Radiology, University of North Carolina, Chapel Hill, NC, USA.

Mailing Address: Richard C. Semelka. The University of North Carolina at Chapel Hill, Campus Box# 7510, 2001 Old Clinic Bldg, Chapel Hill, NC 27599-7510. Email: richsem@med.unc.edu

Received February 5, 2012. Accepted after revision September 11, 2012.

mote control of table motion, together with interconnection of multiple multichannel phased-array coils, has improved the spatial resolution and speed of data acquisition, and rendered whole-body MRI diagnostically accurate and fast[3–5]. It remains important, however, to select the diseases that are of interest for screening because it is still not practicable to study the entire body with dedicated high-spatial-resolution MR sequences due to time constraints.

Other authors have shown the usefulness of whole-body MRI to screen for a variety of diseases, mostly evaluating vessels with MR angiography technique, and in the detection of metastatic cancer[6–12]. These strategies, however, do not evaluate the whole body in a comprehensive fashion for the majority of important diseases, including cancer, vascular and degenerative/inflammatory diseases.

Therefore, the aim of our study was to prospectively evaluate the feasibility of a comprehensive, less than 40 minutes, whole-body MRI protocol, employing a combination of sequences to evaluate a full range of disease processes on a 48-channel 3.0T MR system, with the injection of intravenous gadolinium-based contrast and multiple interconnected regional coils. We describe the strengths of this approach, and the areas where further work is necessary.

MATERIALS AND METHODS

Patients

The study population was comprised of 4 individuals (3 males and 1 female; age range of 28–50 years; mean age of 40 years). Signed informed consent was obtained in accordance with the Institutional Review Board requirements. All subjects were healthy, worried well individuals undergoing screening procedure.

Imaging technique

All MR studies were performed on a new generation 3T MR scanner equipped with 48 channels (Skyra; Siemens, Malvern, PA). A 20-channel head/neck coil, two 18-channel body arrays, and a 32-channel spine array were employed in all subjects.

Patients were supine and placed head first in the scanner. Sequences employed were either breath hold or breathing independent.

The protocol was designed to screen for cancer, vascular disease and inflammatory/degenerative diseases. A combination of single-shot echo-train spin-echo (SS-ETSE) T2-weighted sequences, three-dimensional gradient-echo (3D-GE) T1-weighted pre- and post-gadolinium sequences, with fat-suppression (FS) images, and a fluid attenuated inversion recovery (FLAIR) sequence (head only) were employed. Four regional stations were acquired in the following order: abdomen, chest, pelvis, head and neck. The sequences parameters and the order of sequence acquisition in the four stations are showed in Table 1.

The abdominal images were acquired before and after intravenous administration of 0,1 mmol/kg of gadobenate dimeglumine (MultiHance; Bracco Diagnostics Inc.,

Table 1 Whole-body MRI protocol.

Region	Sequence	Plane	TR (ms)	TE (ms)	Flip (degrees)	Slice thickness (mm)	FOV (mm)	Matrix (pixels)
Abdomen	Localizer							
	T2 SS-ETSE	Coronal	1600	95	130	5.0	450	290 × 320
	T1 3D GE FS	Coronal	4.3	1.8	9	1.5	450	260 × 320
	T2 SS-ETSE FS	Axial	1600	95	160	7.0	380	320 × 240
	T1 3D GE Dixon	Axial	4.5	1.3	9	3.0	380	320 × 250
	T1 3D GE FS pre	Axial	4.3	1.9	9	3.0	380	320 × 260
	→ 20 ml of gadobenate dimeglumine, intravenous injection at 2 ml/sec.							
	T1 3D GE FS arterial	Axial	4.3	1.9	9	3.0	380	320 × 260
	T1 3D GE FS venous	Axial	4.3	1.9	9	3.0	380	320 × 260
	T1 3D GE FS interstitial	Axial	4.3	1.9	9	3.0	380	320 × 260
	T1 3D GE FS	Coronal	4.3	1.8	9	1.5	450	260 × 320
Chest	Localizer							
	T1 3D GE FS	Coronal	4.3	1.8	9	1.5	450	260 × 320
	T1 3D GE FS	Axial	4.3	1.9	9	3.0	380	320 × 260
	T2 SS-ETSE FS	Axial	1600	95	160	5.0	380	320 × 240
	T2 SS-ETSE FS	Coronal	1600	95	130	5.0	450	290 × 320
Pelvis	Localizer							
	T1 3D GE FS	Coronal	4.3	1.8	9	1.5	450	260 × 320
	T1 3D GE FS	Axial	4.3	1.9	9	2.0	380	320 × 260
	T2 SS-ETSE FS	Axial	1600	95	160	5.0	380	320 × 240
	T2 SS-ETSE	Sagittal	1600	95	160	5.0	380	240 × 320
Head and neck	Localizer							
	T1 3D GE FS (head)	Axial	4.3	2.0	9	1.0	280	260 × 320
	T1 3D GE FS (head and neck)	Sagittal	4.3	2.0	9	1.0	380	312 × 384
	T2 SS-ETSE FS (head and neck)	Sagittal	1600	96	160	3.0	400	240 × 320
	FLAIR (head)	Axial	9000	81	150	4.0	220	310 × 320

T2 SS-ETSE, T2-weighted single-shot echo-train spin-echo; T1 3D GE, T1-weighted three-dimensional gradient-echo; FS, fat-suppressed; FLAIR, fluid attenuated inversion recovery.

Princeton, NJ, USA). Abdominal post-contrast images were acquired during the hepatic arterial dominant phase, portal venous phase and hepatic interstitial phase[13]. All sequences of other stations were acquired after intravenous contrast had been administered.

Image analysis

All images of the different anatomical regions were retrospectively evaluated by two radiologists, with 16 years and greater than 20 years experience with MRI, respectively. Both readers independently reviewed all exams evaluating the image quality and the ability of this MRI technique to evaluate mass lesions, metastases or vascular disease of major vessels. The MR image evaluation included: 1) the overall image quality; and 2) comparative assessment of image quality with a priori knowledge of gold standard diagnostic imaging studies. This approach is similar to the approach used by several groups to assess image quality, both for similar applications and more generally[7,9,14–17].

A checklist (Table 2) was created for the overall image quality assessment. Following this checklist, image quality of each station were subjectively graded in terms of diagnostic evaluation for cancer, vascular and degenerative/inflammatory diseases using a 4-point scale, as follows: 1 = poor; 2 = fair; 3 = good; 4 = excellent.

For the comparative assessment rating, the diagnostic image quality of each station was compared with the diagnostic quality of optimal imaging studies on MR (abdomen, pelvis, head and neck) or CT (chest) based on the previous knowledge of two experienced radiologists. Each set of images was then subjectively graded using another 4-point scale, where a score of 1 = poor quality, not diagnostic, a score of 2 = moderately inferior but still adequate quality, a score of 3 = slightly inferior but adequate quality, and a score of 4 = equivalent to optimal quality diagnostic studies.

Kappa (κ) analysis was performed to determine the extent of agreement between the two readers. The level of agreement was defined by κ values as follows: < 0, no agreement; 0–0.40, poor agreement; 0.41–0.75, good agreement; and 0.76–1.0, excellent agreement.

RESULTS

None of the subjects in this study had a prior history of malignancy. Abnormalities detected included liver cysts (1 subject), kidney cysts (2 subjects), degenerative disc disease (2 subjects) and benign prostatic hyperplasia (1 subject). No subject demonstrated lung/chest, brain abnormalities or major vascular disease, nor did any demonstrate a malignancy.

The "in bore" magnet time of studies ranged from 30 to 44 minutes (mean, 38 minutes).

The image quality for cancer was rated as excellent in the brain, lungs, liver, pancreas, kidneys, pelvic organs and rectum, rated as good in bone structures and rated as fair in the esophagus, small bowel and colon, and breast. For vascular diseases ratings were excellent in the aorta and major branches origins, iliac vessels, superior/inferior vena cava, hepatic portal system, hepatic veins and renal veins, and rated as good in pulmonary arteries (successful for the main vessels and at least second order branches), carotid arteries and intracranial vessels, but poor for the coronary arteries. For degenerative/inflammatory disease, ratings were excellent in the brain, liver and pancreas, good in bone structures (spine, hip joints and shoulder joints), and rated as fair in the heart and lungs. The agreement between the two readers for the overall image quality ratings was excellent (κ = 1.0).

For the diagnostic image quality comparison with reference dedicated exams of the same region, all studies of the abdomen were rated as 4, and pelvis were rated as 3. Chest, head and neck were rated as 2. No studies were rated as 1 in any region. The inter-observer agreement was excellent (κ = 1.0). Figures 1–4 show representative images illustrating the standard image quality of the sequences employed in this study.

DISCUSSION

Screening for major diseases throughout the body has been of interest with imaging studies for at least a decade, following the advent of faster imaging. The problem with most strategies for imaging screening, is that the procedure itself may be risky (whole-body CT, PET and PET/CT) and also most approaches have had limited ability to detect a full range of diseases, since their protocols were individually dedicated to the evaluation of metastases or vascular diseases[6–8,10,18–20].

In this study, a fast MR screening approach that screens for major disease categories of cancer, vascular, and degenerative/inflammatory disease was developed. The results show that using this protocol, images of the abdomen are of high diagnostic

Table 2 Checklist.

Cancer	Vascular diseases	Inflammatory/degenerative
Brain	Intracranial vessels	Brain
Lungs	Carotid arteries	Heart
Liver	Coronary arteries	Lungs
Pancreas	Aorta and major branches origin	Bone structures (spine, shoulder, joints and hip joints)
Kidneys	Hepatic portal system	
Esophagus, small bowel and colon	Hepatic veins	
Rectum	Iliac veins	
Pelvic organs	Superior vena cava, inferior vena cava	
Bone structures		
Breast (female)		

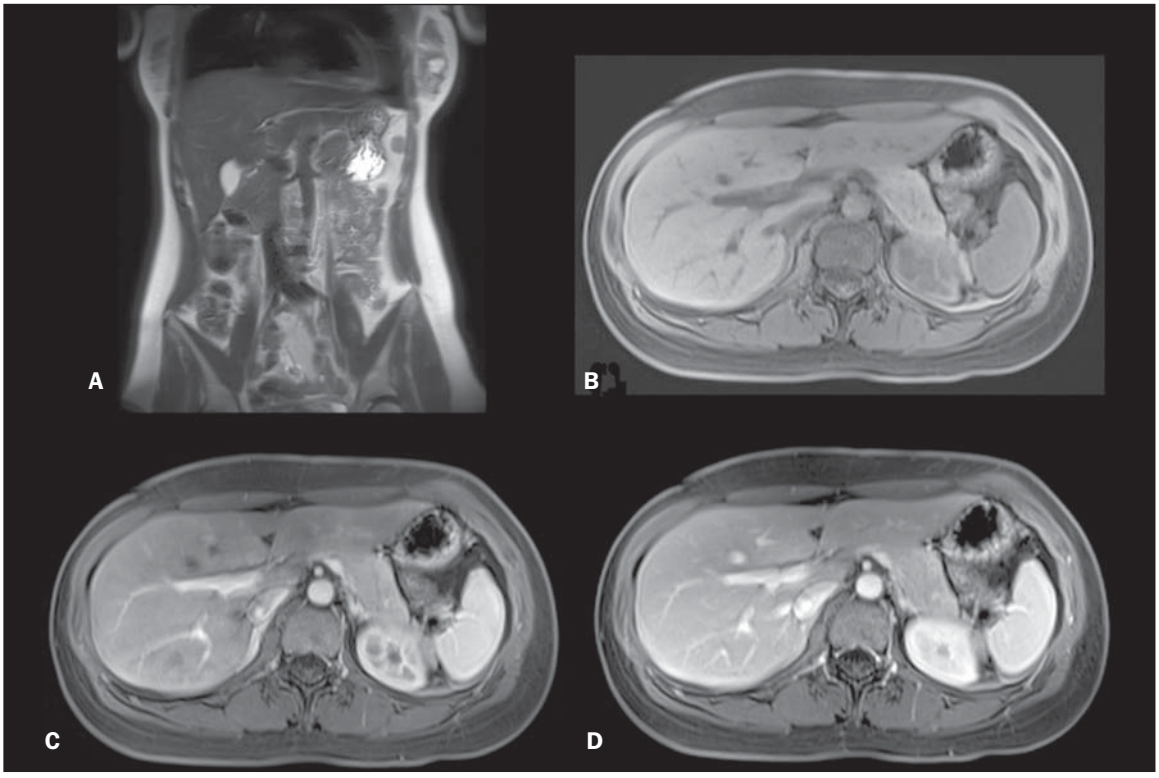

Figure 1. Abdominal region. Coronal T2-weighted single-shot echo-train spin-echo without fat-suppression (**A**), axial T1-weighted 3D gradient-echo fat-suppressed unenhanced (**B**), and gadolinium-enhanced on hepatic arterial dominant phase (**C**) and on interstitial phase (**D**).

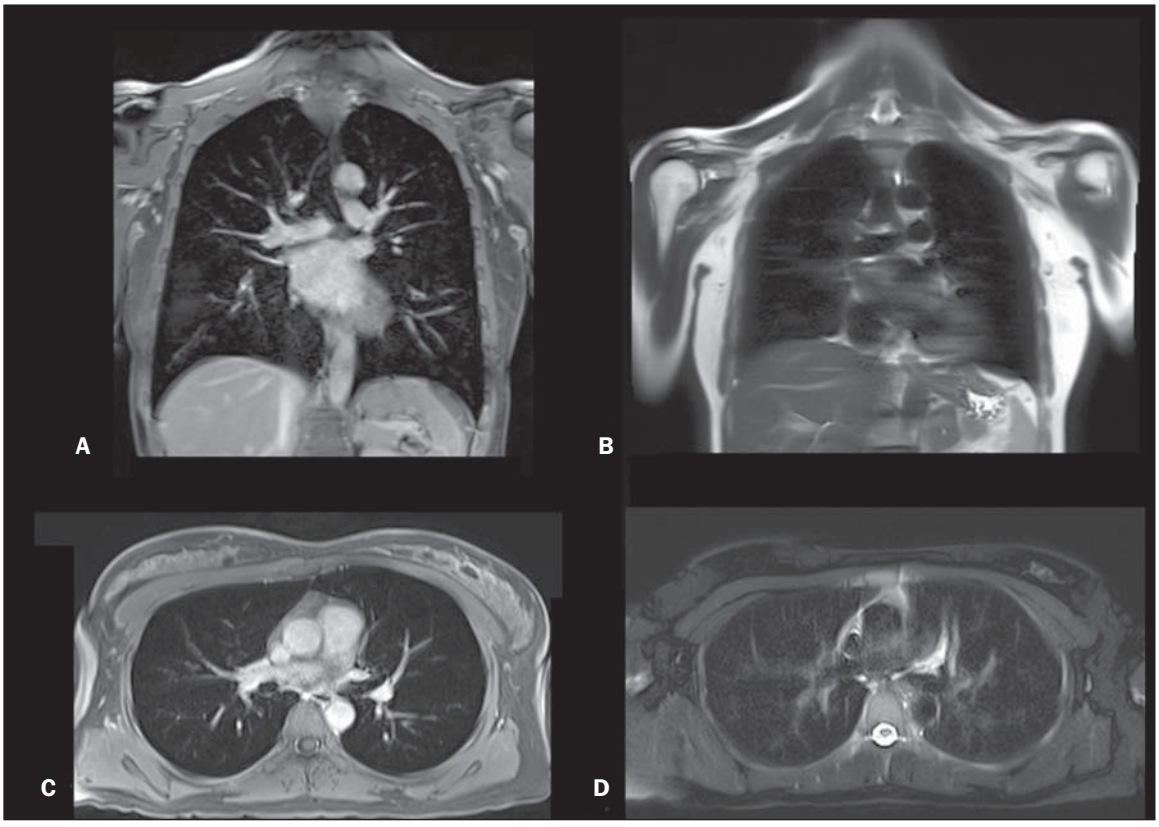

Figure 2. Thoracic region. Gadolinium-enhanced T1-weighted 3D gradient-echo fat-suppressed coronal (**A**) and axial (**C**). T2-weighted single-shot echo-train spin-echo without fat-suppression coronal (**B**) and fat-suppressed axial (**D**).

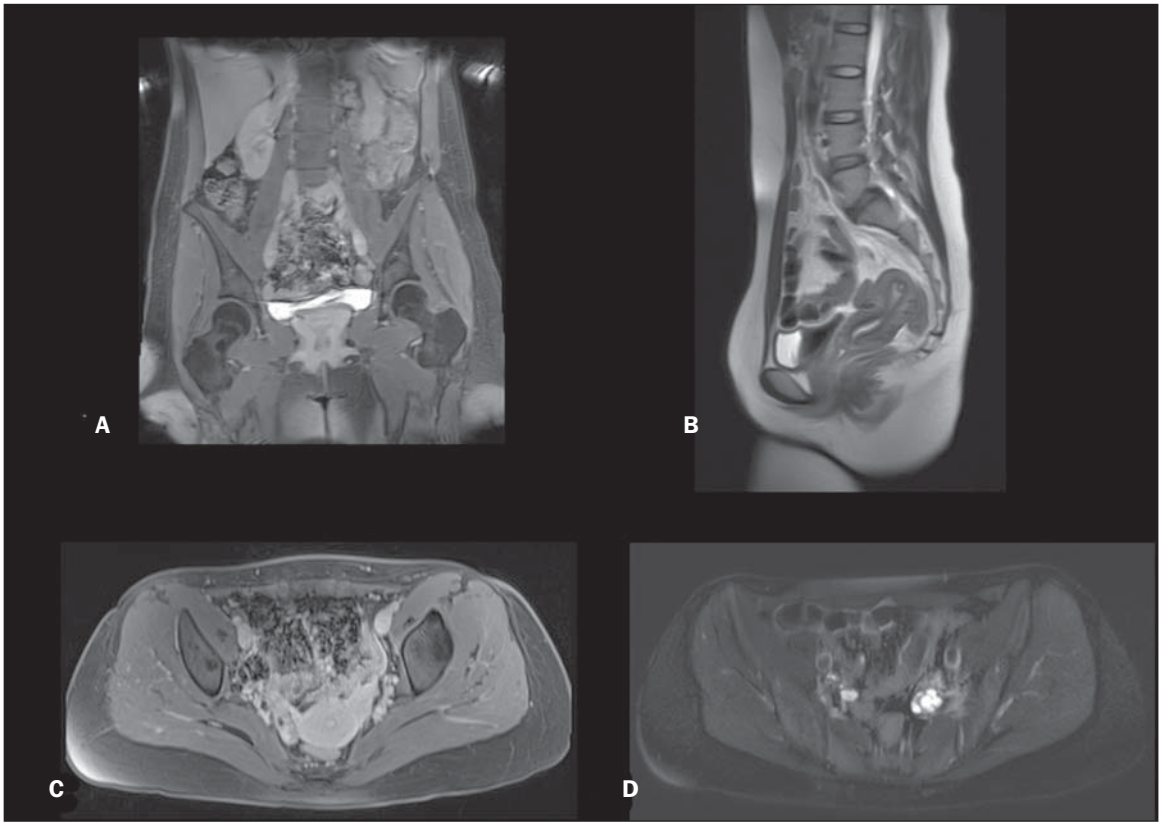

Figure 3. Pelvic region. Gadolinium-enhanced T1-weighted 3D gradient-echo fat-suppressed coronal (**A**) and axial (**C**). T2-weighted single-shot echo-train spin-echo without fat-suppression sagittal (**B**) and fat-suppressed axial (**D**).

quality in all subjects, therefore evaluation of upper abdominal organs with this technique is optimally performed. The abdomen was selected as the first region to be scanned in order to acquire post-contrast hepatic arterial dominant phase images[13], that is the single most important abdominal data set when using nonspecific extracellular gadolinium chelate contrast agent[21]. This technique is essential for imaging the liver, spleen, pancreas, and it provides useful information on the kidneys, adrenals and vessels. Therefore, the timing for this phase of enhancement is the only timing for post-contrast sequences that is crucial.

In the pelvis, sequences of lesser spatial resolution were employed, especially the T2-weighted sequences, compared to optimal dedicated MR pelvic studies[22]. Optimal diagnostic quality T2-weighted sequences are performed with a 512 matrix using a breathing averaged echo-train spin-echo sequence, compared to the 256 matrix of the single-shot T2-weighted echo-train spin-echo in our study, and for this reason pelvic studies were rated as 3 when compared with reference dedicated exams. This protocol is clearly not ideal for small colonic polyps but may be of value for colonic masses greater than 1.0 cm. All pelvic studies demonstrated consistent image quality, which we anticipate that may be adequate to screen for cancer, vascular and degenerative/inflammatory diseases.

MRI of the lung has been limited in the past because of long imaging times, magnetic susceptibility effects and motion artifacts. However, with faster sequences, advanced hardware and high-field-strength MR systems, the image quality has significantly improved. The lack of ionizing radiation exposure make MRI of the lungs ideal for those who must undergo serial imaging, pediatric patients, and as a potential screening tool, which is the aim of our study. One of the sequences used in this protocol was single-shot T2-weighted echo-train spin-echo, since it is generally motion insensitive, has little magnetic susceptibility or phase artifacts, and has been documented to be useful for evaluating the lung parenchyma[9,23,24]. Gadolinium-enhanced images are also necessary for MR assessment of the lungs. The 3D gradient-echo T1-weighted sequence with fat suppression used in this protocol show diminished phase artifact in the retrocardiac region in comparison to two-dimensional gradient-echo T1-weighted images, allowing for better evaluation of all portions of the lung[14,17,25]. The pulmonary vasculature can also be evaluated with this sequence because of its high spatial resolution, which enables high-quality multiplanar reconstruction. Additionally, gadolinium has a larger window of visibility in the pulmonary vessels than iodine on CT images, rendering timing of data acquisition less critical, what is particularly true with the contrast agent employed (gadobenate dimeglumine)[20]. Inflammatory changes in interstitial lung disease, mediastinal and hilar adenopathy, and pulmonary nodules can be evaluated with these two sequences combined[26–31], especially with 3.0 T scanners. Nodules as small as 4 mm can be seen with MRI[28,30,32], and tiny nodules that are missed on MR but seen on CT, are often

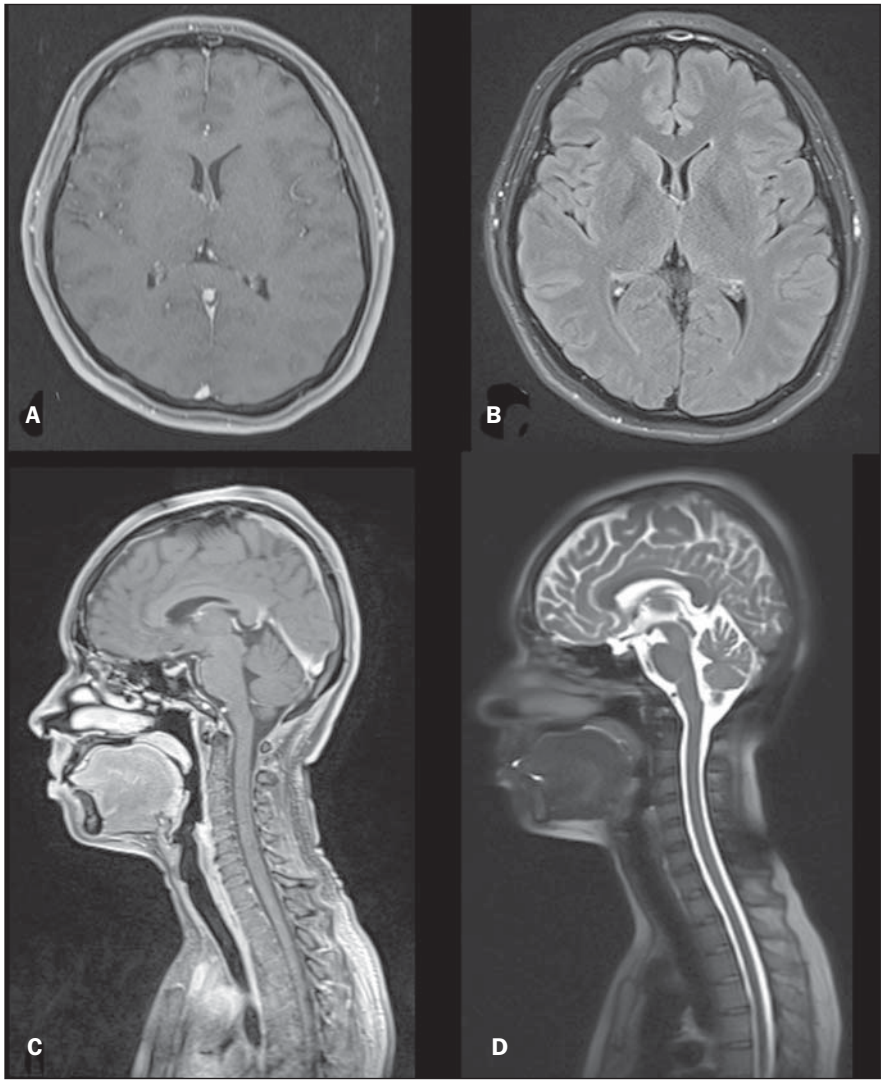

Figure 4. Head and neck regions. Gadolinium-enhanced T1-weighted 3D gradient-echo fat-suppressed axial (**A**) and sagittal (**C**). Axial FLAIR (**B**) and sagittal T2-weighted single-shot echo-train spin-echo fat-suppressed (**D**).

calcified or scarred (fibrotic), showing low proton density and low signal. The chest studies were consistent in image quality, but were rated as 2, using a priori knowledge of CT as comparison because MRI cannot yet depict interstitial lung disease or detect smaller, 2 mm, nodules. However, for the purposes of screening this protocol may be sufficient.

The fat-suppressed 3D gradient-echo sequences used for studying the head and neck, are likely sufficient for mass lesion and inflammatory disease detection, and can be reformatted into different planes if necessary. Less common and more subtle diseases, such as multiple sclerosis plaques, likely would require more sensitive sequences such as FLAIR[33], which was included in our protocol and can also be used for detecting and grading degenerative and microvascular disease, combined with single-shot echo-train spin-echo T2 sequence. Lauenstein et al.[9] reported on the use of gadolinium-enhanced 3D gradient-echo alone in the evaluation of the brain, the addition of the FLAIR and T2-weighted image sequences should provide more complete diagnostic information than they had described.

The neck and carotid arteries were included in this study. The importance of carotid artery disease was the major reason for including the neck. Further optimization may be needed.

Regarding the vascular system, large and medium size vessels were adequately evaluated with post-contrast 3D technique. If the patient has symptomatic vascular disease then it would not be a part of a screening study, but would require a more detailed MR angiographic protocol.

One limitation of this study is the small and healthy study population and the resulting lack of targeted pathology. Thus it should be considered a proof of concept study. However, the sequences employed here have been used for many years as the core of dedicated high-resolution regional protocols. Therefore, we anticipate that this limitation reflects a truly disease-free patient population rather than a failure of the protocol itself. The lesions detected demonstrated the typical characteristics, conspicuity, and quality expected from these sequences when used as part of a dedicated high-resolution protocol. One potentially more severe limitation of this study is the lack of dedicated cardiac sequences, particularly in light of the fact that heart disease is the most common cause of mortality and morbidity[34]. However, the sequences used in this protocol are sensitive to vascular disease in general. It is reasonable to expect that vascular disease in the coronary arteries is likely to be correlated with vascular disease elsewhere[35]. This screening protocol is not recommended for patients with any specific indications of heart disease, and a patient with such indication may require a follow-up with a dedicated cardiac imaging exam.

This proof of concept study shown that comprehensive whole-body MRI exams can be performed in a less than 40-minute period. Based on the experience of the primary investigator the completeness of diagnostic interrogation was considered as follows. The abdominal sequences employed resulted in fully diagnostic studies. Our technique of breast MRI was limited because it did not include serial thin section imaging to generate enhancement curves. However it did show morphological detail, which is important for breast imaging[36] and also can reveal dilated veins that have been reported as consistently present in breast cancer[37]. It should also be feasible to add a more dedicated breast MR study, including a second injection of

gadolinium contrast. No dedicated cardiac sequences were employed. Therefore, patients with suspected heart disease may require a follow-up with dedicated cardiac imaging exam. 3.0T MRI has been shown to demonstrate 4 mm pulmonary nodules consistently, which is sufficient for detection of primary cancer and also sufficient for metastases. This protocol is likely not effective for interstitial lung disease. For patients with specific disease or a strong suspicious, more detailed studies would be required for: colon cancer, breast cancer and coronary artery disease.

In summary, our preliminary results show that a comprehensive whole-body MRI study can be acquired in less than 40 minutes. Both for this study, and for other whole-body screening approaches the strengths and weaknesses should be acknowledged and described to patients.

REFERENCES

1. Semelka RC, Armao DM, Elias J Jr, et al. Imaging strategies to reduce the risk of radiation in CT studies, including selective substitution with MRI. J Magn Reson Imaging. 2007;25:900–9.
2. Brenner DJ, Hall EJ. Computed tomography – an increasing source of radiation exposure. N Engl J Med. 2007;357:2277–84.
3. Griswold MA, Jakob PM, Heidemann RM, et al. Generalized autocalibrating partially parallel acquisitions (GRAPPA). Magn Reson Med. 2002; 47:1202–10.
4. Pruessmann KP, Weiger M, Scheidegger MB, et al. SENSE: sensitivity encoding for fast MRI. Magn Reson Med. 1999;42:952–62.
5. Sodickson DK, McKenzie CA, Li W, et al. Contrast-enhanced 3D MR angiography with simultaneous acquisition of spatial harmonics: a pilot study. Radiology. 2000;217:284–9.
6. Barkhausen J, Quick HH, Lauenstein T, et al. Whole-body MR imaging in 30 seconds with real-time true FISP and a continuously rolling table platform: feasibility study. Radiology. 2001;220: 252–6.
7. Brauck K, Zenge MO, Vogt FM, et al. Feasibility of whole-body MR with T2- and T1-weighted real-time steady-state free precession sequences during continuous table movement to depict metastases. Radiology. 2008;246:910–6.
8. Horvath LJ, Burtness BA, McCarthy S, et al. Total-body echo-planar MR imaging in the staging of breast cancer: comparison with conventional methods – early experience. Radiology. 1999; 211:119–28.
9. Lauenstein TC, Goehde SC, Herborn CU, et al. Whole-body MR imaging: evaluation of patients for metastases. Radiology. 2004;233:139–48.
10. Schmidt GP, Schoenberg SO, Reiser MF, et al. Whole-body MR imaging of bone marrow. Eur J Radiol. 2005;55:33–40.
11. Lauenstein TC, Semelka RC. Emerging techniques: whole-body screening and staging with MRI. J Magn Reson Imaging. 2006;24:489–98.
12. Nava D, Oliveira HC, Luisi FA, et al. Whole-body magnetic resonance imaging for staging and follow-up of pediatric patients with Hodgkin's lymphoma: comparison of different sequences. Radiol Bras. 2011;44:29–34.
13. Goncalves Neto JA, Altun E, Elazzazi M, et al. Enhancement of abdominal organs on hepatic arterial phase: quantitative comparison between 1.5- and 3.0-T magnetic resonance imaging. Magn Reson Imaging. 2010;28:47–55.
14. Bader TR, Semelka RC, Pedro MS, et al. Magnetic resonance imaging of pulmonary parenchymal disease using a modified breath-hold 3D gradient-echo technique: initial observations. J Magn Reson Imaging. 2002;15:31–8.
15. Lauenstein TC, Freudenberg LS, Goehde SC, et al. Whole-body MRI using a rolling table platform for the detection of bone metastases. Eur Radiol. 2002;12:2091–9.
16. Lauenstein TC, Goehde SC, Herborn CU, et al. Three-dimensional volumetric interpolated breath-hold MR imaging for whole-body tumor staging in less than 15 minutes: a feasibility study. AJR Am J Roentgenol. 2002;179:445–9.
17. Semelka RC, Cem Balci N, Wilber KP, et al. Breath-hold 3D gradient-echo MR imaging of the lung parenchyma: evaluation of reproducibility of image quality in normals and preliminary observations in patients with disease. J Magn Reson Imaging. 2000;11:195–200.
18. Domingues RC, Carneiro MP, Lopes FCR, et al. Whole-body MRI and FDG PET fused images for evaluation of patients with cancer. AJR Am J Roentgenol. 2009;192:1012–20.
19. Walker R, Kessar P, Blanchard R, et al. Turbo STIR magnetic resonance imaging as a whole-body screening tool for metastases in patients with breast carcinoma: preliminary clinical experience. J Magn Reson Imaging. 2000;11:343–50.
20. Nael K, Fenchel M, Krishnam M, et al. High-spatial-resolution whole-body MR angiography with high-acceleration parallel acquisition and 32-channel 3.0-T unit: initial experience. Radiology. 2007;242:865–72.
21. Semelka RC, Helmberger TK. Contrast agents for MR imaging of the liver. Radiology. 2001;218: 27–38.
22. Brown ED, Kubik-Huch RA, Reinhold C, et al. Uterus and cervix. In: Semelka RC, editor. Abdominal-pelvic MRI. 2nd ed. Hoboken, NJ: Wiley-Liss; 2006. p. 1251–331.
23. Hatabu H, Gaa J, Tadamura E, et al. MR imaging of pulmonary parenchyma with a half-Fourier single-shot turbo spin-echo (HASTE) sequence. Eur J Radiol. 1999;29:152–9.
24. Yamashita Y, Yokoyama T, Tomiguchi S, et al. MR imaging of focal lung lesions: elimination of flow and motion artifact by breath-hold ECG-gated and black-blood techniques on T2-weighted turbo SE and STIR sequences. J Magn Reson Imaging. 1999;9:691–8.
25. Karabulut N, Martin DR, Yang M, et al. MR imaging of the chest using a contrast-enhanced breath-hold modified three-dimensional gradient-echo technique: comparison with two-dimensional gradient-echo technique and multidetector CT. AJR Am J Roentgenol. 2002;179:1225–33.
26. Kim HY, Yi CA, Lee KS, et al. Nodal metastasis in non-small cell lung cancer: accuracy of 3.0-T MR imaging. Radiology. 2008;246:596–604.
27. Vogt FM, Herborn CU, Hunold P, et al. HASTE MRI versus chest radiography in the detection of pulmonary nodules: comparison with MDCT. AJR Am J Roentgenol. 2004;183:71–8.
28. Yi CA, Jeon TY, Lee KS, et al. 3-T MRI: usefulness for evaluating primary lung cancer and small nodules in lobes not containing primary tumors. AJR Am J Roentgenol. 2007;189:386–92.
29. Chung MH, Lee HG, Kwon SS, et al. MR imaging of solitary pulmonary lesion: emphasis on tuberculomas and comparison with tumors. J Magn Reson Imaging. 2000;11:629–37.
30. Schäfer JF, Vollmar J, Schick F, et al. Detection of pulmonary nodules with breath-hold magnetic resonance imaging in comparison with computed tomography. Rofo. 2005;177:41–9.
31. Hasegawa I, Eguchi K, Kohda E, et al. Pulmonary hilar lymph nodes in lung cancer: assessment with 3D-dynamic contrast-enhanced MR imaging. Eur J Radiol. 2003;45:129–34.
32. Biederer J, Schoene A, Freitag S, et al. Simulated pulmonary nodules implanted in a dedicated porcine chest phantom: sensitivity of MR imaging for detection. Radiology. 2003;227:475–83.
33. Herskovits EH, Itoh R, Melhem ER. Accuracy for detection of simulated lesions: comparison of fluid-attenuated inversion-recovery, proton density-weighted, and T2-weighted synthetic brain MR imaging. AJR Am J Roentgenol 2001;176: 1313–8.
34. Anderson RN, Smith BL. Deaths: leading causes for 2002. Natl Vital Stat Rep. 2005;53:1–89.
35. Kafetzakis A, Kochiadakis G, Laliotis A, et al. Association of subclinical wall changes of carotid, femoral, and popliteal arteries with obstructive coronary artery disease in patients undergoing coronary angiography. Chest. 2005;128:2538–43.
36. Schnall MD, Blume J, Bluemke DA, et al. Diagnostic architectural and dynamic features at breast MR imaging: multicenter study. Radiology. 2006;238:42–53.
37. Sardanelli F, Fausto A, Menicagli L, et al. Breast vascular mapping obtained with contrast-enhanced MR imaging: implications for cancer diagnosis, treatment, and risk stratification. Eur Radiol. 2007;17 Suppl 6:F48–51.